Electronic structure of in-plane functionalized graphane analog interface

*Pappu, Sanjana[#]; Weiss, Elan; Windl, Dr. Wolfgang**
Department of Materials Science and Engineering, The Ohio State University
Columbus, OH 43210, USA

Abstract:

As research on 2D materials and functionalization of 2D crystals continues, we focus on the effects full functionalization of -H and -CH_3 ligands have on a buckled germanene backbone. The crystal structures of hydrogen-terminated germanene and methyl-terminated germanene are simulated using crystal modeling software to observe the properties of both materials and determine whether forming a junction in an interface is practical. The work function and density of states of each 2D structure are analyzed to confirm if the ligands can work well in an interface. By simulating the crystal structure of 2D graphane analog interface and performing electronic calculations using Density Functional Theory methods, we can understand more about ligand chemistry on interfaces. Computational modeling of the structures provides novel insights into the properties and electronic structures of the materials. Successful theoretical results yield for potential synthesis of the materials to be used in the future for devices.

The University of Texas at Austin, Austin, TX
* To whom correspondence should be addressed:
Department of Materials Science and Engineering, The Ohio State University
Columbus, OH 43210, USA
Email: windl.1@osu.edu

1. Introduction:

1.1 Graphane and 2D Material Field

The concept behind working with 2D materials began with the experimental isolation of graphene, individual sheets of carbon, from graphite. The material is incredibly strong, due to its hexagonal lattice structure and covalent intramolecular bonding. After conducting experiments on graphene, researchers found that the material can conduct immensely high levels of heat and electricity because of its sp^2 hybridization.[1] The free π-electrons are delocalized and therefore conduct electricity well when the material is exposed to a current. In addition, the lattice is completely flat, providing little to no resistance for moving electrons, so they pass easily along the surface. For these reasons, graphene is almost too conductive for practical applications. However, this sparked an interest in the field to find novel materials that are still thin, but can be tailored to exhibit different properties. Scientists discovered ways to hydrogenate the carbons in graphene and produce an sp^3 hybridized polymer known as graphane.

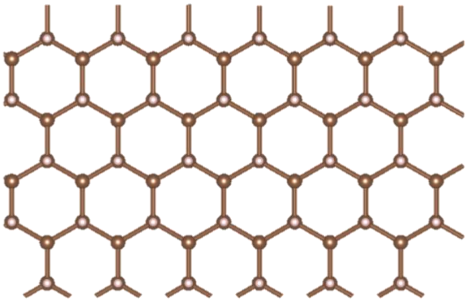

Fig. 1. Hexagonal lattice structure of graphane viewed from c-axis. Brown atoms represent carbon, while pink atoms represent hydrogen.

The new C-H bond ties down the delocalized π-electrons and to form a new σ-bond.[2] Because of its larger band gap, graphane exhibits insulating properties while still retaining thinness, strength, and flexibility. This displays the ability for materials to be modified using chemistry to exhibit desired electronic properties.

1.2 Lateral Interfaces

2D materials have properties that make them unique from 3D bulk materials. The single to few atom thick structures not only allow for thin, flexible sheets, but also tend to be more conductive. It is difficult for current to flow vertically in bulk perpendicular materials, but it flows easily along in-plane lateral materials due to the relative lack of resistance. Modeling an interface instead of a homogenous 2D sheet allows for the electronic properties to be modified even further. The heterogeneous structure has a junction where the material changes from one to the other. The existence of the junction between the two materials give the interface unique electronic properties that can be observed through band bending, a result of a charge imbalance.

1.3 Density Functional Theory

All crystal structures that are simulated are relaxed in VASP (Vienna Ab-initio Simulation Package). VASP performs Density Functional Theory (DFT) calculations on the structures. DFT is a computational modeling technique to investigate the electronic structures of atoms and molecules. The DFT method obtains an approximate solution to the time independent Schrödinger equation of the system using electron density functionals, which speed up calculations.

$$\frac{-h^2}{2m}\frac{\partial^2\Psi(x)}{\partial x^2}+U(x)\Psi(\mathrm{x})=E\Psi(\mathrm{x})$$

Fig. 2. Time-independent Schrödinger equation.

2. Materials and Methods:

2.1 Materials

All crystal structures are generated using CrystalMaker and VESTA (Visualization for Electronic and STructural Analysis) crystal modeling software. Cells are relaxed in VASP using DFT methods.

2.2 Hydrogen Functionalized Germanene

A hydrogen functionalized germanene unit cell is modeled and relaxed using a PBE exchange-correlation functional. An initial (11 x 11 x 11) k-point mesh is used. After relaxation, the dimensions of the cell are a = b = 4.048 Å and c = 6.684 Å.

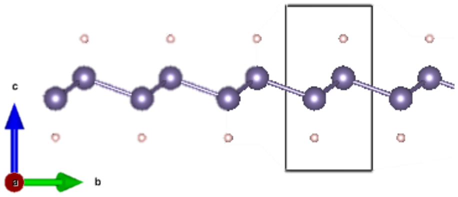

Fig. 3. Hydrogen terminated germanene showing 2D structure from a-axis. Purple atoms represent germanium.

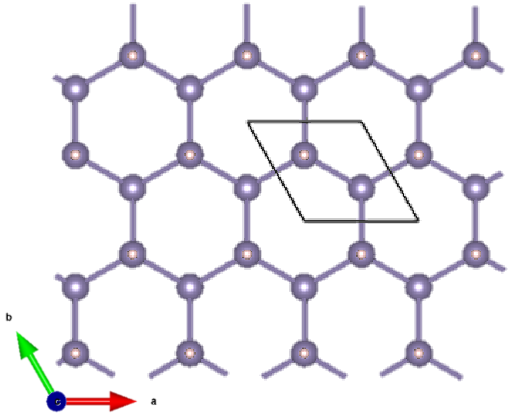

Fig. 4. Hexagonal lattice structure of hydrogen terminated germanene from c-axis.

The k-point mesh is changed to (11 x 11 x 1) after 30 Å of vacuum are added above and below the surface in the c-direction.

2.3 Methyl Functionalized Germanene

The methyl functionalized germanene unit cell is modeled and relaxed using a PBE functional. The same initial k-point mesh used for GeH is used. After relaxation, the dimensions of the cell are a = b = 4.070 Å and c = 15 Å.

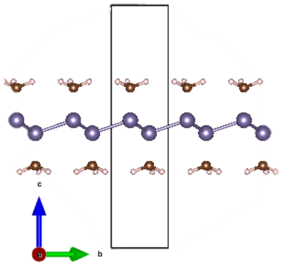

Fig. 5. Methyl terminated germanene showing 2D structure from a-axis.

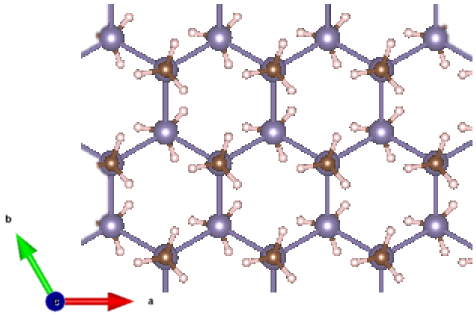

Fig. 6. Hexagonal lattice structure of methyl terminated germanene from c-axis.

The k-point mesh is changed to (11 x 11 x 1) after 20 Å of vacuum are added above and below the surface in the c-direction.

2.4 Germanium Interface

The GeH and $GeCH_3$ structures are used to build the interface. The unit cell contains five layers of methyl-terminated germanene and five layers of hydrogen-terminated germanene. The crystal is relaxed using a PBE exchange-correlation functional. The energy maximum cutoff is set at 400.00 eV and the k-point mesh used is (3 x 11 x 3) to reflect the relatively larger a and c dimensions. After relaxation, the dimensions of the cell are a = 15 Å, b = 4.078 Å, and c = 35.101 Å.

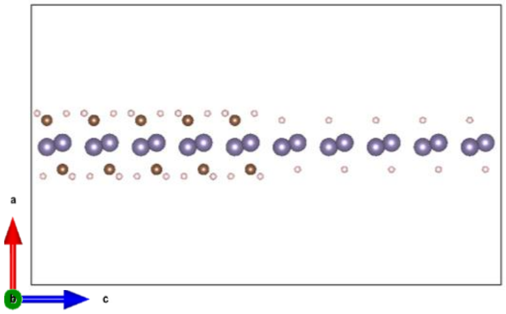

Fig. 7. Functionalized germanene interface showing 2D structure from b-axis. Left five layers are methyl-terminated germanene and right five layers are hydrogen-terminated germanene.

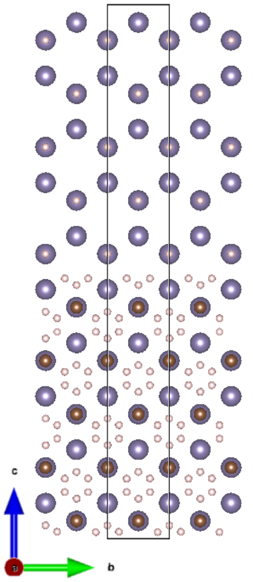

Fig. 8. Hexagonal lattice structure of functionalized germanene interface from a-axis.

3. Results & Discussion:

3.1 Work Function

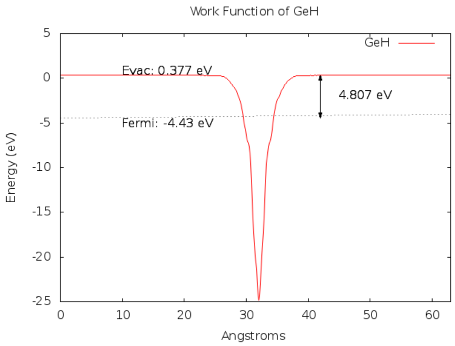

Fig. 9. 2D hydrogen functionalized germanene work function plot with Fermi energy and vacuum levels.

The work function, or electron affinity for nonmetal materials, is defined as the minimum amount of energy required to remove an electron deep within the surface of the material and move it into the free space vacuum.[3] After the initial unit cells are relaxed, additional vacuum is added above and below the material surface so the vacuum level can be calculated in VASP. For hydrogen functionalized germanene, an E_{vac} value of 0.377 eV and a Fermi energy level of -4.43 eV are obtained. The work function depends directly on the vacuum level and Fermi energy value. Subtracting the E_f from the E_{vac} results in a work function value of 4.807 eV, signifying how much energy it takes for an electron to be removed from within the 2D surface.

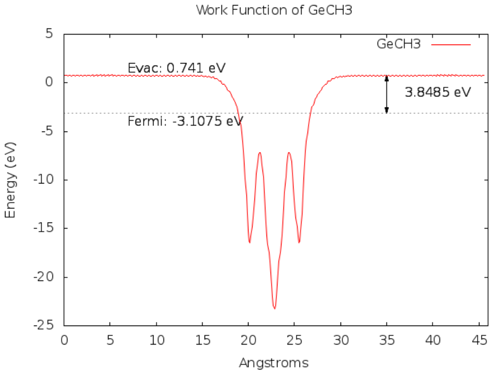

Fig. 10. 2D methyl functionalized germanene work function plot with Fermi energy and vacuum levels.

For methyl functionalized germanene, an E_{vac} value of 0.741 eV and a Fermi energy level of -3.108 eV are obtained, resulting in a work function value of 3.849 eV. This is how much energy it would take for a single electron to be moved from the 2D surface and into the vacuum, a region of lower energy. The work function values for both materials are important in predicting the electronic properties of the interface and the interface junction. The difference between the work function values of the isolated materials is the amount of energy required for electrons to be able to jump the gap and move from the lower conduction band to the conduction band with a higher energy. This difference of 0.959 eV is also significant enough to where it can be predicted there would be some band bending at the interface junction.

3.2 Pure Density of States

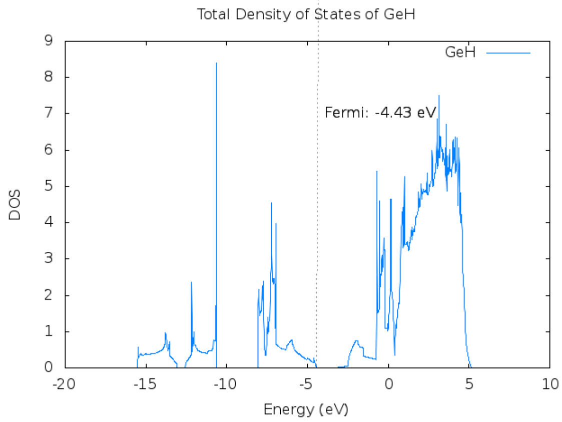

Fig. 11. 2D hydrogen functionalized germanene density of states plot with Fermi energy level.

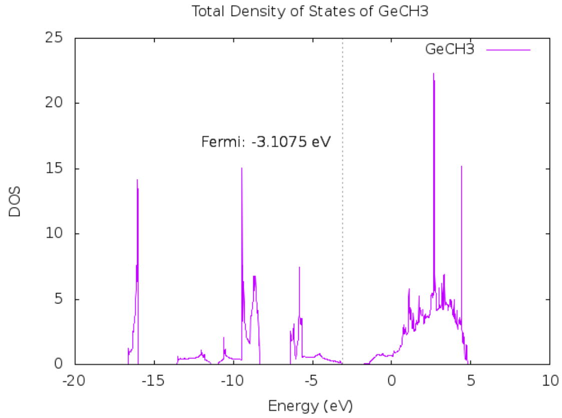

Fig. 12. 2D methyl functionalized germanene density of states plot with Fermi energy level.

The total density of states, defined as the number of different states at an energy level that an electron can occupy, is obtained for both pure materials.[4] The Fermi energy levels are plotted with the DOS to confirm that it is where we would expect – near the valence edge of the band gap of the material. Large spikes in the data represent a high DOS at a specific energy level, meaning there are many states available to be occupied by electrons. The two DOS plots can be compared to see whether the two ligands would work well together in functionalizing an interface. Because both GeH and $GeCH_3$ have a similar band gap, both ligands can functionalize the same backbone in an interface.

3.3 Functionalized Germanene Interface

An interface with a germanium backbone functionalized with -H and $-CH_3$ groups was chosen to be modeled for several reasons. A Ge(111) surface is well established for being able to functionalize ligands due to the properties of germanium.[5] Germanium is more reactive than carbon and is more likely to bond with ligands, especially smaller ones like hydrogen and methyl. Because the arrangement of the germanium atoms in the interface is identical to that of a Ge(111) surface, in which a buckled hexagonal lattice is formed between the atoms, it can be assumed that a germanium backbone would be ideal for observing the electronic properties of multiple ligand functionalization.[5] In addition, the relaxed GeH and $GeCH_3$ unit cells show that the a and b dimensions of both are close enough to where the structures can be used to build the unit cell for the interface.

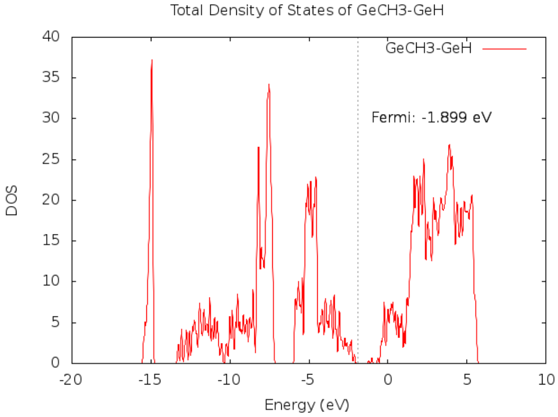

Fig. 13. 2D $-H/-CH_3$ functionalized germanene interface density of states plot with Fermi energy level.

The total density of states is calculated in VASP and plotted to show that, once again, the new Fermi energy level sits on the valence band of the band gap. This time, the DOS data from the interface is used as input to generate the band structure in the 2D heat map. The Fermi energy level of -1.899 eV shows how the valence band edges of pure GeH and $GeCH_3$ shifted once the materials were combined to create a junction at an interface.

3.3 Interface Band Bending

The isolated GeH and $GeCH_3$ materials have different Fermi energy levels, at -4.43 eV and -3.108 eV respectively. Previous literature shows the band gap of GeH is 1.59 eV and the band gap of $GeCH_3$ is slightly larger at 1.82 eV.[6,7]

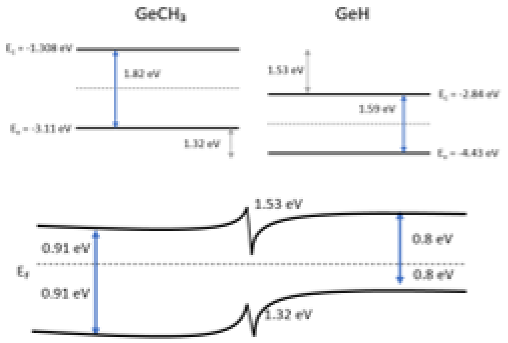

Fig. 14. Isolated conduction/ valence bands for GeH and $GeCH_3$ and predicted band bending when both materials are brought into contact.[8]

However, when the two materials are brought into contact in the interface, the Fermi levels shift to one uniform value in equilibrium.[9] This happens because electrons from the higher Fermi energy level move towards a lower energy level. The recombination of diffused electrons and holes leads to the formation of the depletion region.[9] The valence and conduction bands shift up or down by the same amount, so relative to the Fermi energy level, they are in the same position as before. To see what kind of bending occurs at the junction, however, a 2D heat map is produced.

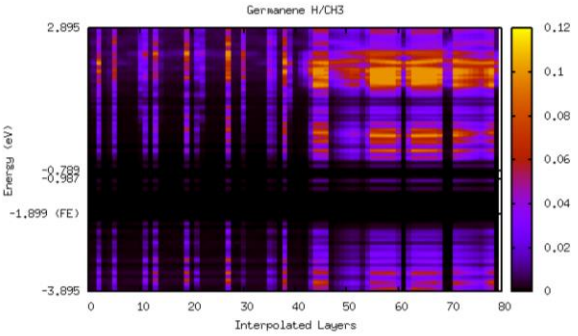

Fig. 16. 2D heat map for -H/-CH_3 functionalized germanene interface showing band structure across a distance and band bending at the junction.

The heat map is required to plot the band structure across a distance because the material is heterogeneous. Unlike a homogeneous structure, a band diagram cannot simply be plotted using the k-points. Band bending indicates that there is a junction in the cell and that the junction has some interesting electronic properties. Bending confirms that modeling an interface with a junction can tailor the electronic properties of the material. However, in this figure, the bending at the junction is not obvious enough.

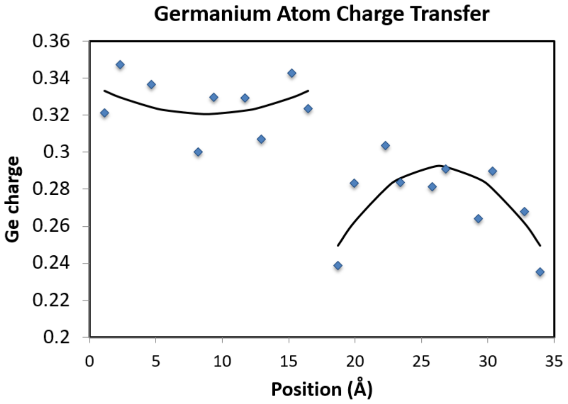

Fig. 17. 2D heat map for -H/-CH_3 functionalized germanene interface showing band structure across a distance and band bending at the junction.

To check whether there is in fact bending at the junction, the Bader charge transfer is plotted for each germanium atom in the backbone of the interface as a function of the atom position in the cell. Two curves are fitted to the data, the left representing the germanium atoms that are functionalized by methyl groups and the right representing the germanium atoms terminated with hydrogen. The reason the charges fall above and below the fitted curve is because the interface plane slightly bent out of place during relaxation. Results are still useful because the curve is fitted. We expect the charges to be more like the curve fit if the plane of the interface is set in place. The GeH charge curve has a steeper slope to it, showing that is bends more. Since it has more bending, this region of the interface has more resistivity and thus induces a voltage drop, confirming that the GeH side of the interface bends downwards at the junction, while the $GeCH_3$ side bends upwards at the junction. This also indicates the existence of a depletion zone that lies mostly on the GeH side of the interface junction.

4. Conclusion:

Analyzing the work function plots and density of states of isolated hydrogen functionalized germanene and methyl functionalized germanene, along with the near identical relaxed unit cell dimensions in the a and b directions, prove that modeling a 2D interface with the two materials is reasonable. A lateral interface allows for better conduction along the surface of the material. Alternatively, bulk material would be far less conductive because of the complications that come with current traveling perpendicular to the interface surface. By analyzing how much charge transfer occurs at each germanium atom of the backbone, we confirm that there is band bending at the junction, most of which occurs in the GeH region. By observing the band bending in the interface junction, we have demonstrated the ability to modify electronic properties of materials. This has significant implications not only for tailoring materials to exhibit desired properties, but also for potential devices in the future.

Research on this structure can continue by using an HSE06 functional in VASP. This functional, although time consuming, yields more accurate calculations for materials with metallic properties because it places the Fermi energy level within the band gap instead of directly above the valence band. To improve charge transfer results, the molecule plane can be set in place during relaxation to ensure that undesired bending of the backbone does not occur. Research on this current topic is not limited to these ligands. We can continue to tailor the electronic properties of the material using other backbones and ligands of various sizes and polarities.[5]

5. Acknowledgements:

I would like to thank Dr. Wolfgang Windl for providing me with a fascinating, novel project and taking the time to meet with me for questions and discussions. In addition, I’d like to extend my thank you to the Windl group for welcoming me into the group and answering any questions I had.

I would also like to thank my graduate mentor Elan Weiss for his patience and for guiding me with my project throughout my REU experience.

Thank you to Michelle McCombs for organizing a wonderful REU experience and my fellow REU students for making these ten weeks unforgettable.

Financial support for this research comes from the National Science Foundation.

6. References:

[1] Woodford, Chris. “Graphene.” *Explain That Stuff.* N.p., 30 Jan. 2017. Web. 27 July 2017.

[2] The University of Manchester. “Scientists Discover Ground-breaking Material: Graphane.” *Phys.org*. N.p., 30 Jan. 2009. Web. 27 July 2017.

[3] Kahn, Antoine. “Fermi Level, Work Function and Vacuum Level.” *Materials Horizons*. The Royal Sociaty of Chemistry, 13 Oct. 2015. Web. 27 July 2017.

[4] “MSE 5317.” *Density of States – MSE 5317*. N.p., n.d. Web. 27 July 2017.

[5] Jiang, Shishi, Kevin Krymowski, Thaddeus Asel, Maxx Q. Arguilla, Nicholas D. Cultrara, Eric Yanchenko, Xiao Yang, Leonard J. Brillson, Wolfgang Windl, and Joshua E. Goldberger. “Tailoring the Electronic Structure of Covalently Functionalized Germanane via the Interplay Ligand Strain and Electronegativity.” *Journal of the American Chemical Society* (n.d.): n.pag. *ACS Publications*. 12 Oct. 2016. Web. 27 July 2017.

[6] Young, Justin R., Basant Chitara, Nicholas Cultrara, and Joshue E. Goldberger. “Water Activated Doping and Transport in Multilayered Germanane Crystals.” *ResearchGate*. N.p., 2011. Web. 27 July 2017.

[7] Jiang, Shishi, Sheneve Butler, Elizabeth Bianco, and Joshua E. Goldberger. “Improving the Stability and Optical Properties of Germanane via One-step Covalent Methyl-termination.” *ResearchGate*. N.p., Feb. 2014. Web. 28 July 2017.

[8] Zeghbroeck, B. Van. “Chapter 4: p-n Junctions.” *P-n Junctions*. N.p., 2011. Web. 27 July 2017.

[9] Kasap, Safa O. “Semiconductor Devices.” *Principles of Electronic Materials and Devices*. Boston: McGraw-Hill, 2002. 434-35. Print.

Materials with Anisotropic Seebeck Behavior for Transverse Thermoelectrics

ERIN R. SNYDER, MIKE SCUDDER, AND JOSHUA E. GOLDBERGER

Alternative energy sources are becoming more desirable to replace other sources that have significant environmental effects or lose a large fraction of the generated energy as waste heat. One solution to this problem is a thermoelectric device, which creates a current from a change in voltage produced by a heat gradient. Typical thermoelectric devices require two separate materials containing different majority carrier types, both p-type and n-type. This allows holes and electrons to travel from the hot end to the cold end, respectively, thereby creating a difference in electrical potential. If one material were able to possess both p-type and n-type behavior in perpendicular axes, as seen through an anisotropic Seebeck coefficient, these devices would offer more practical device engineering as well as geometric adaptability. Several possible candidates were identified by their band structure indicating both p-type and n-type character, including CaAgBi, CaAgSb, CaCuBi, and CaCuSb, and formed using inorganic chemistry crystal synthesis. Phase-pure samples were synthesized by reacting stoichiometric amounts at high temperatures followed by slow cooling and were characterized by X-Ray Diffraction and Raman Spectroscopy. The next step towards transverse thermoelectric devices is creating large, single crystals to find axis dependence in Seebeck coefficients.

Introduction

A modern problem is the creation of an efficient energy source. However, most renewable sources, such as solar, biomass, and wind, have a significant amount of waste heat.[1] One way to improve the efficiency of an energy source is to use heat to supply power. Thermoelectric devices create power through a heat gradient, therefore there is less loss of energy as waste heat.[2]

The first discovery of thermoelectrics was in 1821 when Thomas Johann Seebeck recorded a magnetic field, via a compass, produced from two metals with a temperature difference across a junction.[1] This is called the Seebeck effect, which is now known to be the production of a current due to the movement of holes and electrons from the hot side to the cold side of the system. Similarly, the Peltier effect is the creation of a heat gradient through the application of current to a similar system, used for active cooling in refrigerators.[1]

Typical longitudinal thermoelectric devices use the layer of p-type and n-type materials, which have holes and electrons as charge carriers. With the application of a heat gradient, both holes and electrons move from the warm to the cold side of the materials creating a change in voltage across the system.[2] This voltage difference induces a current, therefore supplying power. These systems are useful not only for their recycling of waste heat, but sustainability, as shown through their continued use in satellites and space probes.[1]

To improve the efficiency of thermoelectrics, the materials must be able to easily conduct electricity. However, in order to maintain the heat gradient the materials should have a low thermal conductivity. The Seebeck coefficient indicates the induced voltage difference for a heat gradient; the larger this number the more effective the thermoelectric device.[3] By combining these values, a material can be quantified as efficient for thermoelectrics.

Longitudinal thermoelectric devices work with the layering of two types of materials. Transverse thermoelectric devices are created using one material with varying Seebeck coefficients based on the angle.[4] This anisotropic Seebeck behavior is created by a material being capable of conducting holes or being p-type in one direction, and conducting electrons or being n-type in the orthogonal direction.[5]

This project examines known materials with properties that may indicate the sample is capable of creating a transverse thermoelectric devices, and attempting to create a pure phase. The synthesized materials are characterized using X-Ray diffraction, which identifies the unit cell and components within it, and Raman spectroscopy, which identifies the vibrational modes within a layered material. Pure phases can be tested for their conductive properties using transport measurements. If the materials are capable of being made in pure phase and conducting electricity the next step is to create large single crystals to record angle dependent Seebeck coefficients and even make a device.

Experimental

Synthesis

The three components were massed and combined in a 1:1 stoichiometric ratio, with a 5 percent carbon excess, in an argon-filled glovebox. All elements were added to a small quartz inner tube and a larger quartz outer tube connected to a vacuum sealing adapter. The tube was connected to a vacuum apparatus and lowered to 70 to 80 mTorr. Using a hydrogen and oxygen torch flame, the quartz tube was sealed.

Sealed tubes were put into a single zone furnace and heated to 1100 ^{o}C at a rate of 358 ^{o}C per hour. Once at this temperature, the tubes dwelled for 12 hours before cooling back down to 25 ^{o}C at a rate of 7 ^{o}C per hour. These tubes were returned to a glovebox and broken open for observation for crystalline facets.

Characterization

Using a mortar and pestle the samples were reduced to a fine powder, then X-ray diffraction was run in an air free beryllium sample holder. Polarized and non-polarized Raman was run on large facets. Then, the powders were compressed into large pellets to run transport measurements to observe ohm’s law.

Results and Discussion

Using the experimental X-ray diffraction patterns compared to known patterns, the purity of the tertiary phases can be determined. Once the phase is achieved, Raman spectroscopy of the materials can also identify the phase and show the layers within. Then, the powder pellets were used to observe ohms' law relationships through transport measurements. Using these tests, it is possible to determine whether these materials are ideal for transverse thermoelectrics.

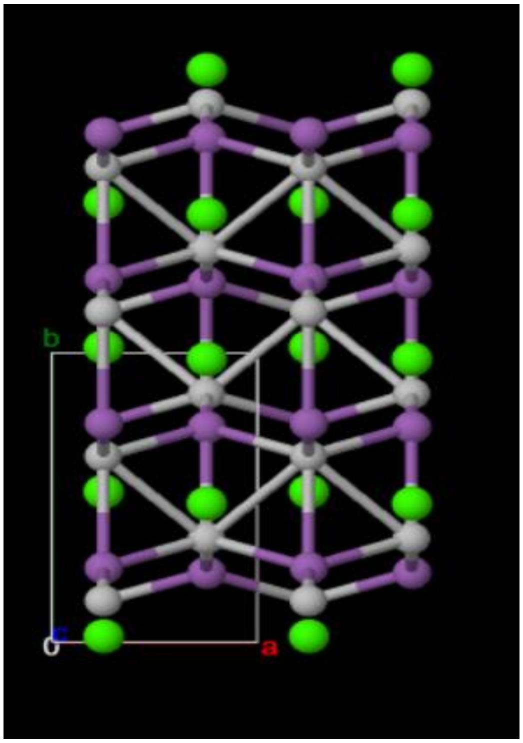
CaAgSb

Figure 1: The space group of CaAgSb is shown as Pnma, produced by the Materials Project.

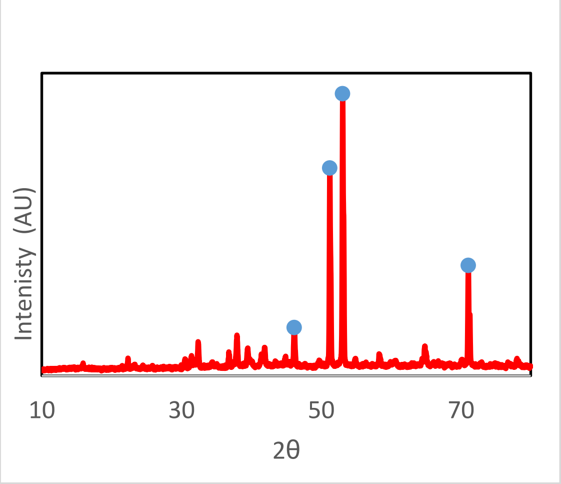

Figure 2: Experimental X-Ray diffraction pattern for synthesized CaAgSb in beryllium sample holder.

Through comparisons using CrystalMaker, the phase for CaAgSb appears to be pure, aside from peaks from the beryllium sample holder.

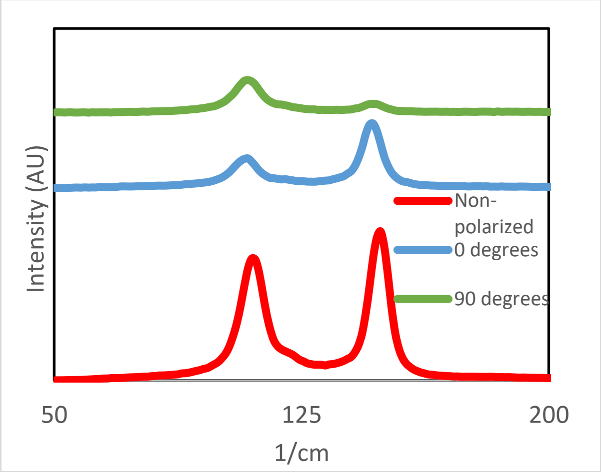

Figure 3: Experimental polarized and non-polarized Raman spectroscopy for synthesized CaAgSb.

Through comparisons of the non-polarized and polarized Raman, the in plane and cross plane modes of CaAgSb can be identified, meaning the material is layered.

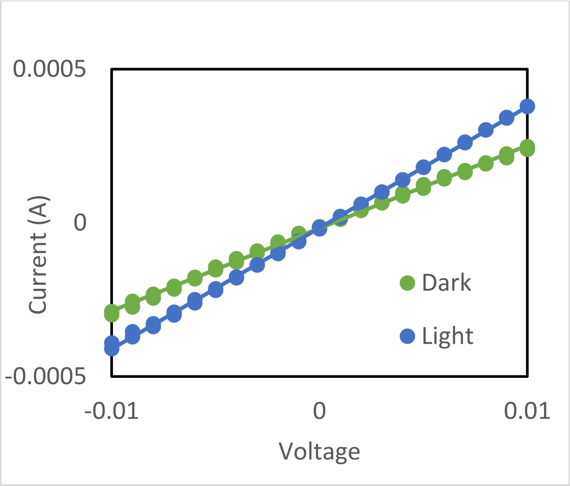

Figure 4: Experimental resistivity measurements in light and dark of synthesized CaAgSb.

The plot of CaAgSb transport measurements follows ohm's law, and indicated that the material is a semiconductor. The increase in slope under illumination indicates an increase in current through the sample in response to the light, a characteristic of semiconductors.

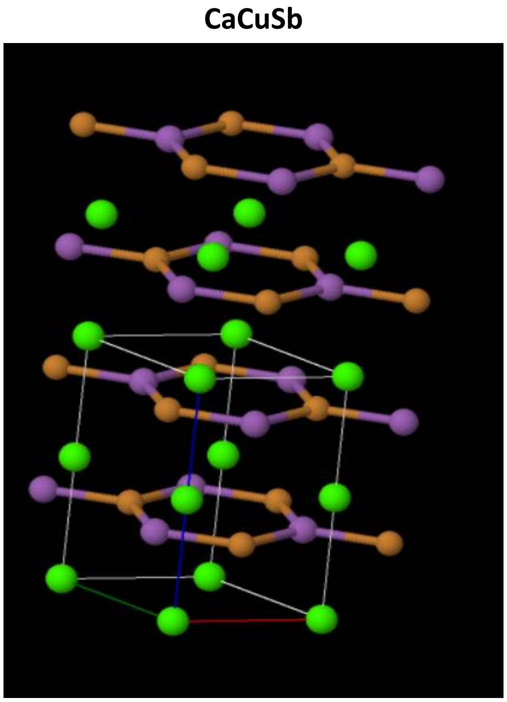

Figure 5: The space group of CaCuSb is shown as $P6_3/mmc$, produced by the Materials Project.

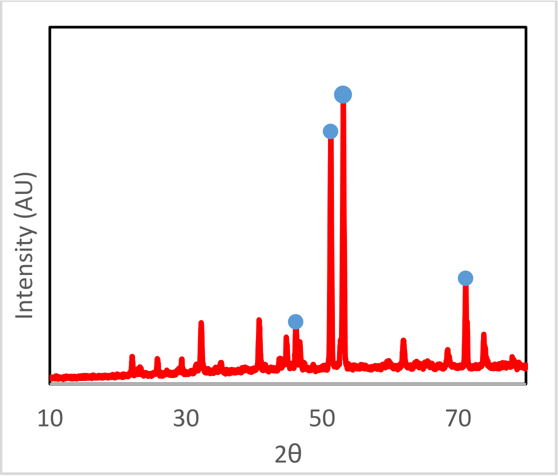

Figure 6: Experimental X-Ray diffraction pattern for synthesized CaCuSb in beryllium sample holder.

The sample of CaCuSb, ran in an air free sample holder, was identified as pure through comparison to known patterns.

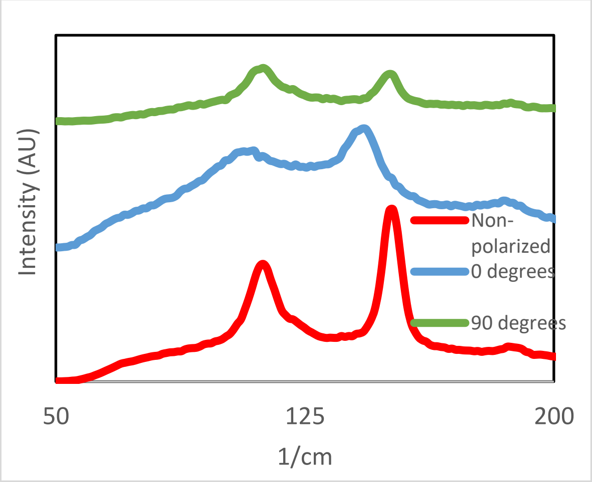

Figure 7: Experimental polarized and non-polarized Raman spectroscopy for synthesized CaCuSb.

The polarized Raman of CaCuSb shows the layered structure of the pure phase when compared to the non-polarized, by exciting the orthogonal vibrational modes.

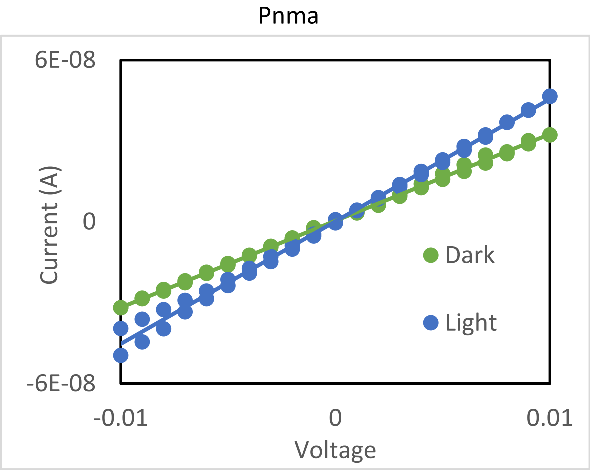

Figure 8: Experimental resistivity measurements in light and dark of synthesized CaCuSb.

The comparative plot of dark versus light transport measurements identifies CaCuSb as a semiconductor due to the increase in resistivity, or slope, with the addition of light.

CaCuBi

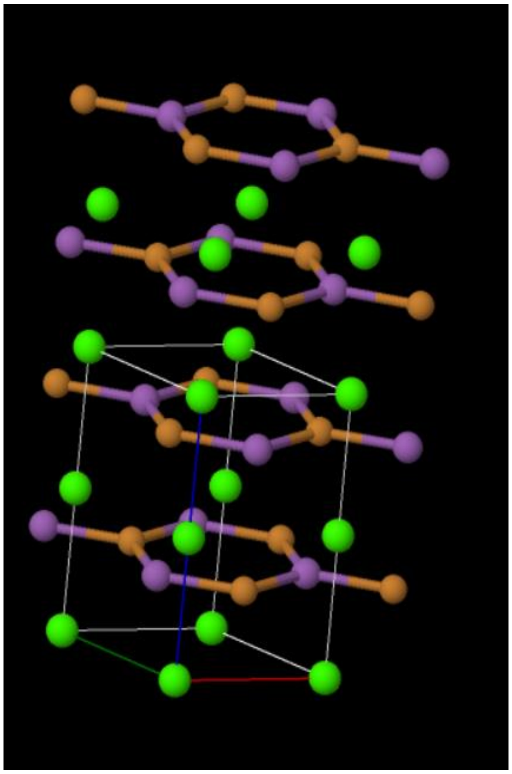

Figure 9: The space group of CaCuBi is shown as, P6$_3$/mmc produced by the Materials Project.

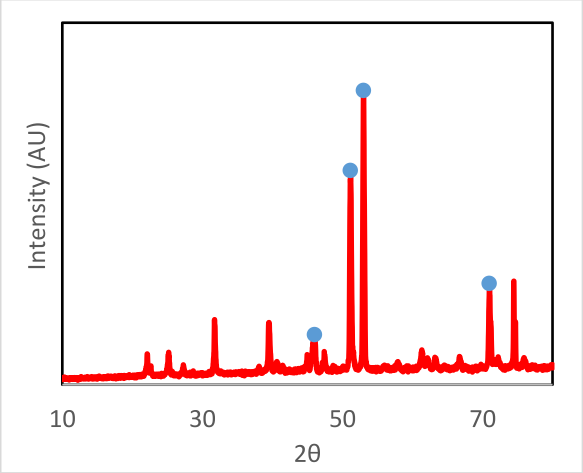

Figure 10: Experimental X-Ray diffraction pattern for synthesized CaCuBi beryllium sample holder.

The X-ray diffraction pattern of synthesized CaCuBi shows a pure phase, other than peaks identified for the beryllium sample holder.

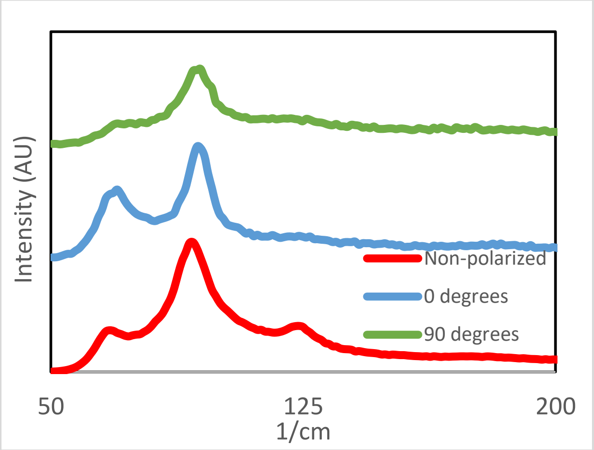

Figure 11: Experimental polarized and non-polarized Raman spectroscopy for synthesized CaCuBi.

By observing polarized Raman of CaCuBi, variation in peak intensities indicates a layered material. However, the peak present only in the non-polarized Raman may result from the heavy element Bismuth present.

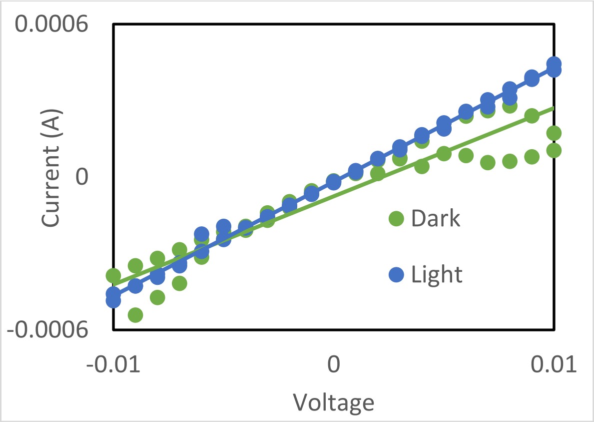

Figure 12: Experimental resistivity measurements in light and dark of synthesized CaCuBi.

Comparing the light and dark measurements of CaCuBi, the resistivity of the material increases when exposed to light. This qualifies the material as a semiconductor. Comparatively, CaCuBi in the dark has a less linear trend than the other materials.

CaAgBi

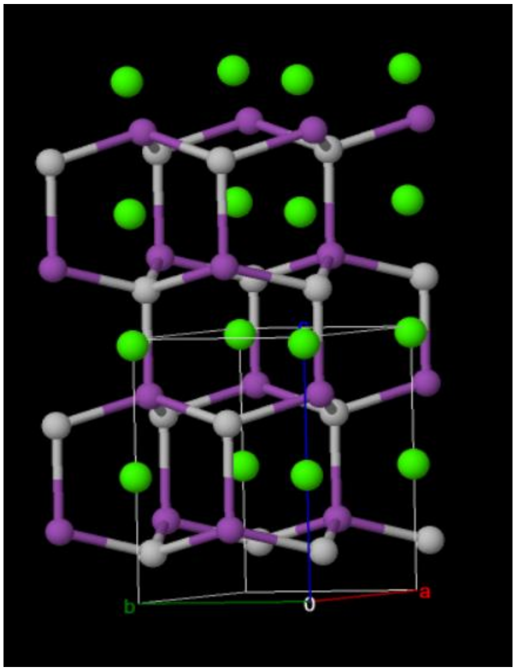

Figure 13: The space group of CaAgBi is shown as $P6_3mc$, produced by the Materials Project.

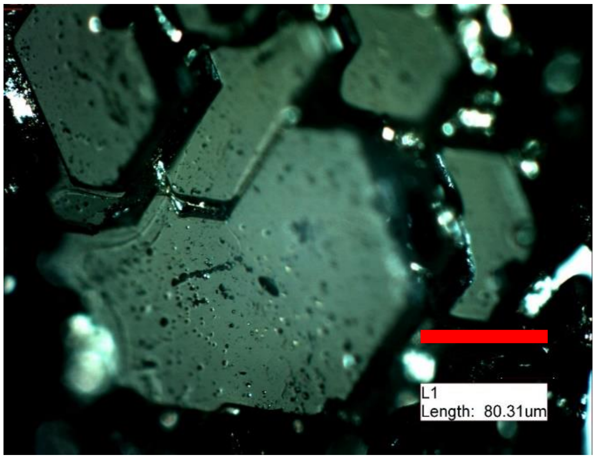

Figure 14: Hexagonal crystal facet of synthesized CaAgBi at 10x magnification.

The facet on the CaAgBi crystal supports the creation of a pure materials since the hexagonal shape matches the space group's 6 point symmetry. This facet indicates that the growth of large single crystals is possible.

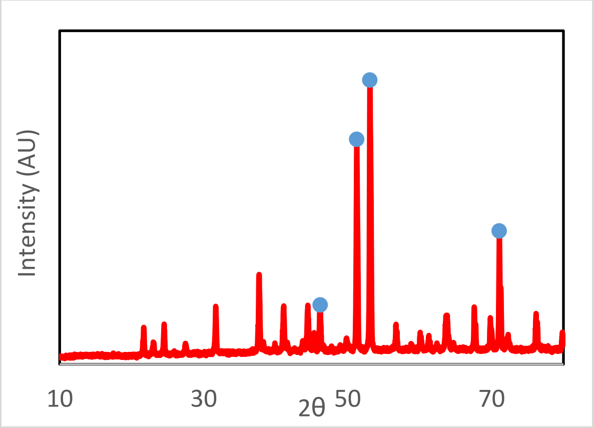

Figure 15: Experimental X-Ray diffraction pattern for synthesized CaAgBi in beryllium sample holder.

Synthesized CaAgBi was identified as pure by comparing the known material X-ray diffraction to the experimental.

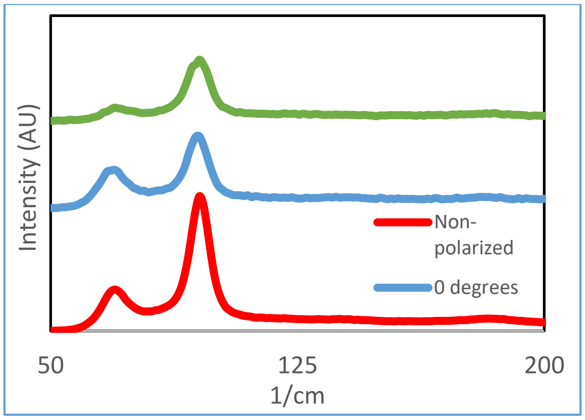

Figure 16: Experimental polarized and non-polarized Raman spectroscopy for synthesized CaAgBi.

Raman spectroscopy compares the polarized and non-polarized to identify layers within a material. By exciting the materials along two different axis in polarized Raman, the peaks due to in plane or cross plane bonds can be seen in the spectra.

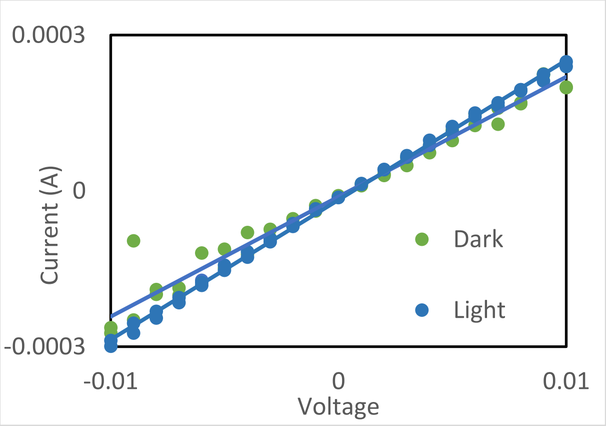

Figure 17: Experimental resistivity measurements in light and dark of synthesized CaAgBi.

The transport measurements of CaAgBi show that the sample conducts electricity, and the material is a semiconductor.

All the samples indicate that they were capable of making pure tertiary phase, shown through comparison of experimental versus known X-ray diffraction patterns. The Raman spectroscopy compares non-polarized and polarized spectroscopy to identify in plane and out of plane vibrations. These materials appear to have layers, making them ideal for angle dependent, or anisotropic behavior. Lastly, the transport measurements aim to show the resistivity of the material, seen as the slope. The ohm's law relationship and similarity between conduction in light and dark indicates that the materials are all semiconductors with near zero band gaps.

Conclusion

CaCuBi, CaCuSb, CaAgBi, and CaAgSb are materials with achievable layered pure phases that conduct electricity. The four materials were characterized as phase-pure via X-Ray Diffraction and were shown to exhibit structural anisotropy via Raman Spectroscopy. Transport measurements indicated that each sample was also conductive. As a result, these materials have potential for use in a transverse thermoelectric device. Proceeding forward with these experiments, the next step would be to produce large single crystals to acquire Seebeck coefficient measurement along varying axes. Then, using promising materials a transverse thermoelectric device can be created.

References

1. Zhang, X.; Zhao, L. Thermoelectric materials: Energy conversion between heat and electricity. *Journal of Materiomics* DOI:10.1016/j.jmat.2015.01.001. 2015, *1*(2), 92–105.
2. Snyder, J. G.; Toberer, E. S. Complex thermoelectric materials. *Nature Materials* DOI: 105-114. DOI:10.1038/nmat2090. 2008, *7*, 105–114.
3. Sootsman, J. R.; Chung, D. Y.; Kanatzidis, M. G. ChemInform Abstract: New and Old Concepts in Thermoelectric Materials. *ChemInform* DOI:10.1002/chin.200952221. 2009, *40*(52).
4. Tang, Y.; Cui, B.; Zhou, C.; Grayson, M. P × n-Type Transverse Thermoelectrics: A Novel Type of Thermal Management Material. *Journal of Electronic Materials* DOI: 10.1007/s11664-015-3666-z. 2015, *44*(6), 2095–2104.
5. Goldsmid, H. J. Application of the Transverse Thermoelectric Effects. *Journal of Electronic Materials* DOI:10.1007/s11664-010-1357-3. 2010, *40*(5), 1254–1259.